ARTICLES

Hydrodynamic theory of density relaxation in near-critical fluids

Didier Bailly[1] and Bernard Zappoli[2]

[1]*ONERA, 29 Avenue de la Division Leclerc, 92322 Châtillon Cedex, France*
[2]*CNES, 18 Avenue Edouard Belin, 31055 Toulouse Cedex, France*

This paper gives a complete hydrodynamic theory of density relaxation after a temperature step at the boundary of a cell filled with a nearly supercritical pure fluid in microgravity conditions. It uses the matched asymptotic expansion technique to solve the one-dimensional Navier-Stokes equations written for a viscous, low-heat-diffusing, near-critical van der Waals gas. The continuous description obtained for density relaxation in space and time confirms that it is governed by two fundamental mechanisms, the piston effect and heat diffusion. It gives a space-resolved description of density inside the cell during the divergently long heat diffusion time, which is shown to be the ultimate one to achieve complete thermodynamic equilibrium. On that very long time scale, the still measurable density inhomogeneities are shown to follow the diffusion of the vanishingly small temperature perturbations left by the piston effect. Temperature, which relaxes first to nonmeasurable values, and density, which relaxes on a much longer time scale, may thus appear to be uncoupled. The relaxation of density on the diffusion time scale is shown to be driven by a bulk expansion-compression process slowly moving at the heat diffusion speed, which is generated by heat diffusion coupled with the large compressibility of the near-critical fluid. The process is shown to be the signature of the thermoacoustic events that occur during the very short piston effect time period. The generalization of the theory to real critical behavior opens the present results to future experimental investigation.

PACS number(s): 64.70.Fx, 65.70.+y, 68.35.Rh, 81.70.Ha

I. INTRODUCTION

It is widely admitted now that heat can propagate much faster than it would by simple diffusion in a convection-free near-critical pure fluid owing to a fourth mechanism of heat transport named the piston effect or adiabatic effect [1–4]. This effect corresponds to the adiabatic compression of the bulk phase caused by mass addition into the bulk from the heated, very compressible, initial thermal boundary layer, which therefore experiences a strong mass depletion. A number of experiments have been performed recently in weightless conditions to check and study this heat transfer process extensively [5–10]. However, attention was soon drawn to the fact that density relaxation was, on the contrary, a very slow process. This was mentioned very early by Onuki and Ferrel [10] who found a long tail in the density relaxation process and gave a characteristic time for density relaxation that is close to the critically slowing down heat diffusion time. At the same time several experiments also reported a very long density equilibration time, while temperature was already quite homogeneous. Guenoun *et al.* [4] reheated phase-separating CO_2 to above its critical temperature and observed, through interferometric images, that the significant density inhomogeneities slowly relaxed diffusively after the piston effect had adiabatically homogenized the temperature. More recently, Zhong and Meyer [8,11] have studied the transient density changes after boundary heating and have clearly shown that the relaxation time diverges after the sharp response during the adiabatic transfer of energy from the boundary region to the bulk fluid by the piston effect.

Boukari, Pego, and Gammon [12] studied the dynamics of the gravity-induced density profile near the liquid-vapor critical point. They studied the dynamics of the density profile formation that follows a temperature quench at the lower boundary of a horizontal, infinite, critical xenon layer (the upper boundary being cooled more slowly to avoid convective instabilities) in great detail to give a reliable model for interpreting earth-bound experiments. In the same way, they report that, while temperature is practically homogenized by the piston effect after some tenths of a second, the density profile changes over a time scale of hours, that is to say, very slowly. Of course the one-dimensional (1D) downward gravity-induced advective flow enhances the equilibration in that case, but the order of magnitude of a diffusive process still holds. The relaxation of a density gradient caused by applying an electrostriction volume force has also been explored recently [13] and shown to occur diffusively. Zimmerly *et al.* [14], have studied the role of convection in temperature and density relaxation. They show that, under earth gravity conditions, the piston effect is still responsible for temperature equilibration since it homogenizes temperature before convection has time to start. Convection is then triggered in a practically thermally homogeneous medium by the still large density gradients remaining after the piston effect has played its role. This direct Navier-Stokes simulation pointed out the leading role played by density relaxation, which rules out the long-lasting, quasi-isothermal convective motion that follows boundary heating. This current interest in density relaxation in near-critical fluids stems from the fact that, owing to the diverging compressibility, density per-

turbations are still significant and accessible to experiments on a time scale over which temperature perturbations are no longer measurable. It should be recalled that the relative temperature and density perturbations differ initially by several orders of magnitude owing to the diverging compressibility. Accordingly, when temperature has relaxed to nonmeasurable values by the piston effect, density perturbations are, in relative order, still as large as the temperature ones were at the early stages of the process. The theory of density relaxation in near-critical pure fluids thus deserves, beyond the early formal theoretical work by Onuki and Ferrel [10], an extensive theoretical analysis similar to what has been done for temperature relaxation. The early, fast piston effect period has been extensively studied. No such theory exists for the next period of time when the still significantly nonhomogeneous density field relaxes to complete equilibrium, coupled with temperature perturbations that are several orders of magnitude smaller. In particular, no space-resolved description of density relaxation to complete equilibrium exists today. We therefore develop in this paper the Navier-Stokes theory of density relaxation which follows a boundary temperature increase of a near-critical fluid cell. This done with two main aims. The first is to obtain an asymptotically matched analytical solution of the Navier-Stokes equations that provides scaling for space, time, and physical properties and which is continuously valid in space and time from the beginning of the heating to complete equilibrium. To achieve this, we show the classical description of the fast adiabatic heat equilibration, previously obtained on the piston effect time scale, to be nonuniform in space when time becomes infinite with respect to that time scale. This makes it necessary to rescale time and introduce the heat diffusion time scale to overcome this singularity and to achieve the matching of the two time scales. A set of equations is then obtained for this divergently long time scale, which is solved by the Laplace transform technique. It is shown in particular that density is governed by a diffusion equation that reflects the diffusion of asymptotically small temperature inhomogeneities. These inhomogeneities are the remains of the initial perturbations left in place by the piston effect in a time frame when both processes, the piston effect and heat diffusion in the bulk phase, give comparable contributions to the evolution. The present approach, which is consistent with the purely thermodynamic early scaling work of Onuki and Ferrell, allows the space structure of the hydrodynamic field to be obtained. The second goal is to explore this structure, from the beginning of the heating to complete equilibrium, with particular emphasis on the long heat diffusion time scale. When the boundary layer ceases to provide the bulk with fluid because temperature is almost homogenized by the piston effect, the density field is made up of a deep depletion of fluid in the vicinity of the heated wall and a homogeneously increased density in the bulk phase. The asymptotic matching procedure gives access to the space structure of these inhomogeneities, which are the initial conditions for the differential equations and thus the key point of the problem. Diffusion is shown to generate a damped expansion-compression process that propagates very slowly at the heat diffusion speed in the bulk and evens out the inhomogeneities. This phenomenon is thus the legacy of the fast thermoacoustic heat transfer period and this particular structure

of density relaxation is another signature of the piston effect. After these theoretical results were obtained, previous raw temperature data obtained by Beysens *et al.* [15] were processed. They studied the thermalization of a near-critical fluid cell set at critical density and 6 mK above the critical point after 5 mW constant power during 15 s heat pulse. Although the boundary conditions differ from those under consideration here, the corresponding temperature evolution exhibits different types of variations with time depending on the location in the cell. These variations show similarities with the present theoretical findings but still need extended analysis. In order to prepare for the interpretation of such experiments, we generalize the theory to real critical exponents. Not only does this formal effort thus give a complete hydrodynamic description of the relaxation of a near-critical fluid but it also leads to insights into density relaxation that were not observed or even expected before.

Section II presents the model; the previously obtained descriptions are recalled and the solution obtained on the heat diffusion time scale. Section III gives a uniformly valid description in space and time from the initial heating to the final equilibrium, and discusses and compares it with the descriptions obtained previously. Section IV is devoted to the discussion of density relaxation on the long diffusive time scale. The results for real critical exponents are given in Secs. V and VI.

II. MODEL

The model presented here is similar to those used in our previous theoretical work [14,16]. In what follows, the prime denotes dimensional parameters, the subscript "0" denotes the ideal gas, and the subscript "i" denotes the initial conditions.

A 1D (slablike) container is filled with a near-critical van der Waals gas at critical density, initially at rest and at thermal equilibrium, in a zero-g environment. The temperature of the left-hand side wall is raised on a time scale equal to the diffusion time in the perfect gas (some millikelvins in some seconds) and then kept constant; the right-hand sidewall is insulated. The fluid itself is described by the 1D Navier-Stokes equations written for a Newtonian fluid, using the following nondimensional parameters (representing density, temperature, pressure, velocity, time, and space, respectively):

$$\rho = \frac{\rho'}{\rho_c'}, \quad T = \frac{T'}{T_c'}, \quad P = \frac{P'}{\rho_c' r' T_c'}, \quad u = \frac{u'}{\sqrt{\gamma_0 r' T_c'}},$$

$$t = \frac{t'}{t_a'}, \quad x = \frac{x'}{L'}.$$

Here T_c', ρ_c', and P_c' are the critical coordinates, r' is the ideal gas constant R' divided by the molar mass of the gas, and $t_a' = L'/\sqrt{\gamma_0 r' T_c'}$ is the typical acoustic time, equal to 3.3×10^{-5} s for a 10-mm-long sample cell.

This means that time is first referred to the acoustic characteristic time and the length is expressed relative to the width of the slablike sample cell. As stated above, the equation of state used here is the van der Waals equation of state,

which exhibits a $(T'-T'_c)^{-1}$ divergence of the compressibility at the critical point. In a real fluid, the thermal conductivity also diverges. This fact is taken into account by the introduction of the following temperature dependence:

$$\frac{\lambda'}{\lambda'_0}=1+\Lambda\left(\frac{T'-T'_c}{T'_c}\right)^{-1/2}.$$

This results from the mean field theory, which is consistent with the van der Waals model. It has long been known that classical equations of state do not lead to correct critical exponents. However, both the numerical experiments and previous asymptotic analysis [16,17] have already demonstrated that a van der Waals equation can provide rich phenomenological information concerning, for example, the mechanism of interaction of a near-critical thermal plume with a thermostated boundary, while enabling relatively simple calculation [18]. This choice was therefore made to facilitate a formal analysis of the process, rather than a quantitative comparison with real experiments. However, as shown in [6], the calculation based on the van der Waals equation can be extended to real critical exponents because of the linear character of the problem. Real critical exponents are considered in Sec. VI and a generalized theory is given which is shown not to change the phenomenology.

When put into the Navier-Stokes equations, the nondimensional parameters listed above lead to the definition of the following quantities:

$$\varepsilon=\frac{t'_a}{t'_d}Pr_0, \quad \mu=\frac{T'_i-T'_c}{T'_c},$$

where $t'_d=L'^2/\kappa'_0$ is the characteristic diffusion time and κ'_0 the thermal diffusivity of the ideal gas. ε and μ are very small when compared to 1 (for instance, in the case of CO_2 in a 10 mm container, $\varepsilon=3.5\times10^{-8}$). If the specific heat at constant volume is assumed to be constant and equal to that of the ideal gas, the choice for the specific heat at constant pressure is imposed [and thus its $(T'-T'_c)^{-1}$ divergence] since the van der Waals equation of state is considered.

The resulting system of equations is then as follows:

$$\rho_t+(\rho u)_x=0, \tag{1}$$

$$\rho u_t+\rho u u_x=-\frac{1}{\gamma_0}P_x+\frac{4}{3}\varepsilon u_{xx}, \tag{2}$$

$$\rho T_t+\rho u T_x=-(\gamma_0-1)(P+\tfrac{9}{8}\rho^2)u_x$$
$$+\varepsilon\left\{\frac{\gamma_0}{Pr_0}\left[\left(1+\frac{\Lambda}{\sqrt{T-1}}\right)T_{xx}-\tfrac{1}{2}\Lambda T_x^2\right]\right.$$
$$\left.\times(T-1)^{-3/2}\right]+\tfrac{4}{3}\varepsilon\gamma_0(\gamma_0-1)u_x^2\right\}, \tag{3}$$

$$P=\frac{\rho T}{1-\tfrac{1}{3}\rho}-\tfrac{9}{8}\rho^2. \tag{4}$$

The initial conditions are

$$T(t=0)=1+\mu, \quad \rho(t=0)=1,$$

$$P(t=0)=P_i=\tfrac{3}{2}(1+\mu)-\tfrac{9}{8}, \quad u(t=0)=0, \tag{5}$$

and the boundary conditions are

$$T(x=0,t)=1+\mu+\alpha\left[\frac{t}{t_0}-H_{[t_0]}\left(\frac{t}{t_0}-1\right)\right]. \tag{6}$$

Where $H_{[t_0]}$ is the Heaviside step function, equal to zero for t smaller than t_0 and 1 for t greater than t_0. Equation (6) signifies that the maximum-temperature increase $(\alpha T'_c)$ at the boundary is reached for $t'_a t_0$ after a linear increase in time. The order of magnitude of the temperature increases at the boundary is thus proportional to

$$T_x(x=1,t)=0 \quad \text{(thermostated cell)},$$

$$u(x=0)=u(x=1)=0 \quad \text{(rigid boundaries)}.$$

The presence of several small quantities (ε,μ) in the above system suggests that the problem could be treated by an-asymptotic analysis. Since this problem is singular near its boundaries for the condition $\varepsilon\rightarrow0$, we have chosen to use the matched asymptotic expansion technique to solve the above system of equations analytically.

III. PREVIOUS ASYMPTOTIC ANALYSES

A. Acoustic period

As in [7], the asymptotic analysis was first performed on the acoustic time scale and, for the sake of clarity, we recall the basic principles of the procedure used in that reference. The acoustic time scale is the shortest macroscopic time scale the Navier-Stokes equations can describe, and we thus began studying the problem on that time scale. Taking into account the fact that the increase in temperature of the wall occurs on the diffusion time scale in the perfect gas defined by the variable $\tau=\varepsilon t$, which is much longer, the increase in temperature on the acoustic scale is of order ε. The diffusion depth on the acoustic time scale is thus of order $\sqrt{\varepsilon}\mu^{0.25}$ in the supercritical fluid, since the diffusion tends to zero as $\mu^{-0.5}$, whereas it is of order $\sqrt{\varepsilon}$ in an ideal gas. It can be noted now that the heat diffusion time scale in a supercritical pure fluid is defined by $\theta=\varepsilon\sqrt{\mu}t$. Without reporting here on the whole procedure that was used to obtain the solution on the acoustic time scale a procedure that is explained in detail in [16], it is, however, worth giving the solution for the flow-field variables in the thermal boundary layer and in the bulk phase.

The boundary-layer solution, expressed as a function of the rescaled space variable and of the time t, that is to say, the time in units of the acoustic time, is

$$T^a_{BL}=1+\mu+\alpha4\frac{1}{t_0}[ti^2\,\mathrm{erfc}(\eta)$$
$$-H_{[t_0]}(t-t_0)i^2\,\mathrm{erfc}(\eta/\sqrt{1-t/t_0})], \tag{7}$$

$$\rho_{BL}^a = 1 - \frac{\alpha 8}{\mu 3}\frac{1}{t_0}[ti^2\,\mathrm{erfc}(\eta)$$
$$- H_{[t_0]}(t-t_0)i^2\,\mathrm{erfc}(\eta/\sqrt{1-t/t_0})], \qquad (8)$$

$$u_{BL}^a = \frac{\alpha\varepsilon^{1/2}}{\mu^{3/4}}\sqrt{D_c}\frac{1}{t_0}\left[\sqrt{t}\left(\frac{2}{\sqrt{\pi}} - i^0\,\mathrm{erfc}(\eta)\right) - H_{[t_0]}\sqrt{(t-t_0)}\right.$$
$$\left.\times\left(\frac{2}{\sqrt{\pi}} - i^0\,\mathrm{erfc}(\eta/\sqrt{1-t/t_0})\right)\right], \qquad (9)$$

where

$$\eta = \frac{z}{2\sqrt{D_c}\sqrt{t}} = \frac{x/\sqrt{\mu}}{2\sqrt{D_c}\sqrt{t}} \quad \text{and} \quad D_c = \frac{\gamma_0}{\gamma_0-1}\frac{\Lambda}{Pr_0}. \quad (10)$$

Here D_c is a nondimensional coefficient linked to the critical part of the heat diffusivity defined by

$$\kappa' = \frac{\lambda_0'\gamma_o\Lambda}{\rho_c'C_{p0}'(\gamma_0-1)}\sqrt{\mu} = \kappa_0'\frac{\gamma_0\Lambda}{\gamma_0-1}\sqrt{\mu} = \kappa_0'D_c Pr_0\sqrt{\mu}.$$

This last expression is the first-order expansion of the heat diffusivity in the near-critical region:

$$\kappa' = \frac{\lambda_0'(1+\Lambda/\sqrt{\mu})}{\rho_c'C_{p0}'(1+R'/C_{p0}'\mu)},$$

where $R' = C_{p0}'(\gamma_0-1)/\gamma_0$ is the ideal gas constant. Note that, according to the van der Waals theory and the mean field approximation, the heat diffusivity thus tends to zero as $\sqrt{\mu}$.

Considering now that, from Eq. (9),

$$\lim_{z\to\infty} u_{BL}^a = \frac{2}{\sqrt{\pi}}\frac{\sqrt{D_c}}{t_0}[\sqrt{t} - H_{[t_0]}\sqrt{(t-t_0)}], \qquad (11)$$

one can show that this mass addition generates in the bulk phase an acoustic perturbation of magnitude $\alpha\varepsilon^{1/2}/\mu^{3/4}$, which is $\mu^{3/4}$ stronger than in the perfect fluid [16]. The corresponding solution is

$$T_B^a = 1 + \mu + \frac{\alpha\varepsilon^{1/2}}{\mu^{3/4}}\frac{\gamma_0-1}{c_0 t_0}\sqrt{D_c}\left(\frac{4c_0}{3\sqrt{\pi}}[t^{3/2} - H_{[t_0]}(t-t_0)^{3/2}]\right.$$
$$\left.+ \frac{2}{\pi^{3/2}}\sum_{n=1}^{\infty}[S_n'(t,x,0) - H_{[t_0]}S_n'(t-t_0,x,0)]\right),$$

$$\rho_B^a = 1 + \frac{\alpha\varepsilon^{1/2}}{\mu^{3/4}}\frac{1}{3}\frac{\gamma_0-1}{c_0 t_0}\sqrt{D_c}\left(\frac{4c_0}{3\sqrt{\pi}}[t^{3/2} - H_{[t_0]}(t-t_0)^{3/2}]\right.$$
$$\left.+ \frac{2}{\pi^{3/2}}\sum_{n=1}^{\infty}[S_n''(t,x,0) - H_{[t_0]}S_n''(t-t_0,x,0)]\right),$$

$$(12)$$

$$P_B^a = \frac{3}{2}(1+\mu) - \frac{9}{8} + \frac{\alpha\varepsilon^{1/2}}{\mu^{3/4}}\frac{3}{2}\frac{\gamma_0-1}{c_0 t_0}$$
$$\times\sqrt{D_c}\left(\frac{4c_0}{3\sqrt{\pi}}[t^{3/2} - H_{[t_0]}(t-t_0)^{3/2}]\right.$$
$$\left.+ \frac{2}{\pi^{3/2}}\sum_{n=1}^{\infty}[S_n(t,x,0) - H_{[t_0]}S_n(t-t_0,x,0)]\right),$$

$$u_B^a = \frac{\alpha\varepsilon^{1/2}}{\mu^{3/4}}\frac{\sqrt{D_c}}{t_0}\left(\frac{2}{\sqrt{\pi}}\{(1-x)[t^{3/2} - H_{[t_0]}(t-t_0)^{3/2}]\}\right.$$
$$\left.+ \frac{2}{\pi^{3/2}}\sum_{n=1}^{\infty}[C_n(t,x,0) - H_{[t_0]}C_n(t-t_0,x,0)]\right).$$

B. Piston effect time scale

When t tends to infinity when expressed in units of acoustic time, the temperature in the bulk, from Eq. (12) for T, becomes

$$T_B \approx 1 + \mu + \frac{\alpha\varepsilon^{1/2}}{\mu^{3/4}}\sqrt{D_c}\left(\frac{4}{3}\frac{\gamma_0-1}{\sqrt{\pi}}\sqrt{t}\right.$$
$$\left.+ \text{bounded acoustic terms}\right) + o\left(\frac{\alpha\varepsilon^{1/2}}{\mu^{3/4}}\right)$$

and thus grows continuously as the square root of time, since the acoustic terms remain bounded following the properties of the Fresnel integrals. In contrast, in the boundary layer, from Eq. (7), the temperature for infinite times counted on the acoustic time scale remains $O(\alpha)$; accordingly there exists a time scale defined by $\tau = \xi t$, with $\xi \ll 1$, for which the temperature in the bulk is of the same order as the temperature in the boundary layer:

$$\frac{\alpha\varepsilon^{1/2}}{\mu^{3/4}}\xi^{-1/2} = \alpha \Rightarrow \xi = \frac{\varepsilon}{\mu^{3/2}} \Rightarrow \tau = \frac{\varepsilon}{\mu^{3/2}}t. \qquad (13)$$

For an ideal gas or a critical fluid far from the critical point, the time scale is simply $\tau = \varepsilon t$. This means that, for a near-critical fluid, the cell is thermalized on a time scale much shorter than the heat diffusion time scale in an ideal gas. The time scale itself is much shorter than the diffusion time in the critical fluid (by a factor $\sqrt{\mu}$). This is the essence of the so-called piston effect or adiabatic effect, the nature of which is thermoacoustic and which allows for a temperature homogenization over a time scale much shorter than diffusion would do. In mathematical terms, it also means that when time (t) tends to infinity on the acoustic time scale, the match on that time scale between the solution for temperature in the bulk and the solution for temperature in the boundary layer is no longer obtained. As a matter of fact, the matching condition between these two solutions is expressed by

$$\lim_{z\to\infty}[T_{BL}^a - (1+\mu)] = \lim_{x\to 0}[T_B^a - (1+\mu)].$$

It is indeed fulfilled when $t = O(1)$, since $\lim_{x \to 0}[T_B^a - (1 + \mu)] = (\alpha \varepsilon^{1/2}/\mu^{3/4}) f(t)$ means that the first perturbation in the bulk is of order $O(\alpha \varepsilon^{1/2}/\mu^{3/4})$, which is zero at the order α and is thus equal to $\lim_{z \to \infty}[T_{BL}^a - (1 + \mu)] = 0$. This condition is no longer fulfilled when $t \to \infty$ since temperature in the bulk increases continuously as $\sqrt{t}$ while temperature in the boundary layer remains of order α. The necessity to rescale time comes from the need to match temperature in the boundary layer and in the bulk for increasing times. When we express that matching for increasing times counted in units of the piston effect characteristic time, we find expression (13) for the characteristic time τ.

The boundary-layer solution for the flow-field variables on the time scale as defined in Eq. (13), which has been presented in [19], is the following:

$$T_{BL}^{PE} = 1 + \mu + \alpha \left[1 - e^{(\gamma_0 - 1)^2 D_e \tau} i^0 \, \mathrm{erfc}[(\gamma_0 - 1)\sqrt{D_c}\sqrt{\tau}] \right.$$
$$+ e^{[(\gamma_0 - 1)\bar{z} + (\gamma - 1)^2 \sqrt{D_c}\sqrt{\tau}]}$$
$$\left. \times i^0 \, \mathrm{erfc}\left((\gamma_0 - 1)\sqrt{D_c}\sqrt{\tau} + \frac{\bar{z}}{2\sqrt{D_c}\sqrt{\tau}} \right) \right]$$
$$= 1 + \mu + \alpha \tilde{T}_{BL}^{PE},$$

$$\rho_{BL}^{PE} = 1 - \frac{\alpha}{\mu} \frac{2}{3} e^{[D_c(\gamma_0 - 1)^2 \tau + (\gamma_0 - 1)\bar{z}]}$$
$$\times i^0 \mathrm{erfc}[(\gamma_0 - 1)\sqrt{D_c}\sqrt{\tau}]$$
$$\times i^0 \mathrm{erfc}\left((\gamma_0 - 1)\sqrt{D_c}\sqrt{\tau} + \frac{\bar{z}}{2\sqrt{D_c}\sqrt{\tau}} \right)$$
$$= 1 + \frac{\alpha 2}{\mu 3} \tilde{\rho}_{BL}^{PE},$$

$$P_{BL}^{PE} = \tfrac{3}{2}(1 + \mu) - \tfrac{9}{8} + \alpha \tfrac{3}{2} \{ 1 - e^{(\gamma_0 - 1)^2 D_c \tau}$$
$$\times i^0 \mathrm{erfc}[(\gamma_0 - 1)\sqrt{D_c}\sqrt{\tau}] \}$$
$$= \tfrac{3}{2}(1 + \mu) - \tfrac{9}{8} + \alpha \tfrac{3}{2} \tilde{P}_{BL}^{PE},$$

$$u_{BL}^{PE} = \frac{\alpha \varepsilon}{\mu^{3/2}} \frac{2}{3} \frac{1}{\sqrt{D_c}} \left\{ \frac{\sqrt{D_c}}{\sqrt{\pi}\sqrt{\tau}} (\gamma_0 - 1) \right.$$
$$\times e^{(\gamma_0 - 1)^2 D_c \tau} \left[e^{(\gamma_0 - 1)\bar{z}} \, \mathrm{erfc}\left((\gamma_0 - 1)\sqrt{\tau} + \frac{\bar{z}}{2\sqrt{D_c}\sqrt{\tau}} \right) \right.$$
$$\left. - \mathrm{erfc}[(\gamma_0 - 1)\sqrt{D_c}\sqrt{\tau}] + \frac{1}{\sqrt{\pi}\sqrt{\tau}}(1 - e^{\bar{z}^2/4D_c\tau}) \right] \right\}$$
$$= \frac{\alpha \varepsilon 2}{\mu^{3/2} 3} \frac{1}{\sqrt{D_c}} \tilde{u}_{BL}^{PE}. \tag{14}$$

The boundary-layer thickness is $O(\mu)$ on that time scale and $\bar{z} = z/\mu$ is the boundary-layer variable.

The solution in the bulk phase is the following:

$$T_B^{PE} = 1 + \mu + \alpha[1 - e^{(\gamma_0 - 1)^2 D_c \tau} i^0 \, \mathrm{erfc}((\gamma_0 - 1)\sqrt{D_c}\sqrt{\tau})],$$

$$\rho_B^{PE} = 1 + \alpha \tfrac{2}{3} \{ 1 - e^{(\gamma_0 - 1)^2 D_c \tau} i^0 \, \mathrm{erfc}[(\gamma_0 - 1)\sqrt{D_c}\sqrt{\tau}] \},$$
$$(15)$$
$$u_B^{PE} = \frac{\alpha \varepsilon 2}{\mu^{3/2} 3} \sqrt{D_c} \left(\frac{1}{\sqrt{\pi}\sqrt{\tau}} - (\gamma_0 - 1)\sqrt{D_c} \right.$$
$$\left. \times i^0 \mathrm{erfc}[(\gamma_0 - 1)\sqrt{D_c}\sqrt{\tau}] \right) (1 - x).$$

From solutions (14) and (15), respectively, in the boundary layer and in the bulk, it is possible to obtain a uniformly valid expression in space which is valid on the piston effect time scale by employing the classical additive composition procedure. This procedure consists in forming, for any dependent variable, the function

$$X^{PE}(x, \tau) = X_{BL}^{PE}\left(\frac{x}{\mu}, \tau \right) + X_B^{PE}(x, \tau) - \lim_{x/\mu \to \infty, x \ll 1} X_{BL}^{PE}\left(\frac{x}{\mu}, \tau \right),$$

so that, by invoking the matching condition,

$$\lim_{x/\mu \to \infty, x \ll 1} X_{BL}^{PE}\left(\frac{x}{\mu}, \tau \right) = \lim_{x \to 0} X_B^{PE},$$

one can check that the function $X(x, \tau)$ is uniformly valid at the first order (ε) throughout the whole domain. The uniformly valid description of the flow field as given in [19] is the following:

$$p(\tau) = p_B^{PE},$$

$$T^{PE} = T_{BL}^{PE}\left(\frac{x}{\mu}, \tau \right),$$

$$\rho^{PE} = \rho_{BL}^{PE}\left(\frac{x}{\mu}, \tau \right),$$

$$u^{PE} = \frac{\alpha \varepsilon}{\mu^{3/2}} \frac{2}{3} \sqrt{D_c} \left\{ (1 - x) \left[\frac{1}{\sqrt{\pi}\sqrt{\tau}} \right. \right.$$
$$\left. - (\gamma_0 - 1)\sqrt{D_c} e^{(\gamma - 1)^2 D_c \tau} \mathrm{erfc}[(\gamma_0 - 1)\sqrt{D_c}\sqrt{\tau}] \right]$$
$$- \frac{e^{-x^2/\mu^2/4D_c\tau}}{\sqrt{\pi}\sqrt{\tau}} (\gamma_0 - 1)\sqrt{D_c} e^{(\gamma_0 - 1)^2 D_c \tau + (\gamma_0 - 1)x/\mu}$$
$$\left. \times \mathrm{erfc}\left((\gamma_0 - 1)\sqrt{D_c}\sqrt{\tau} + \frac{x/\mu}{2\sqrt{D_c}\sqrt{\tau}} \right) \right\}. \tag{16}$$

IV. DENSITY RELAXATION

Equations (14) and (15) give a representation of the phenomena occurring on the piston effect time scale. The solution is classical and has been written in the case of different boundary heating or sometimes under different formulations that are nearly equivalent. However, these solutions cannot describe the evolution to final equilibrium since we presently

show that it is nonuniform in space when time tends to infinity on the piston effect time scale. It is thus necessary, in order to fulfill the matching condition at all length scales, to introduce a new time scale, which proves to be the heat diffusion time scale.

A. The density relaxation time scale

When time tends to infinity on the piston effect time scale, that is to say, when $\tau \to \infty$, solution (16) behaves as follows for temperature, pressure, and fluid velocity:

$$T^{PE} \approx 1 + \mu + \alpha - \alpha \frac{1}{\sqrt{D_c}\sqrt{\pi}} \frac{1}{(\gamma_0-1)} \frac{1}{\sqrt{\tau}} (1 - e^{-x^2/4D_c\tau}),$$

$$p^{PE} \approx \frac{3}{2}(1+\mu) - \frac{9}{8} + \alpha \frac{3}{2}\left(1 - \frac{1}{(\gamma_0-1)} \frac{1}{\sqrt{\pi}\sqrt{D_c}\sqrt{\tau}}\right),$$
(17)

$$u^{PE} \approx \frac{2}{3} \frac{\alpha\varepsilon}{\mu^{3/2}} \frac{1}{2\sqrt{\pi}} \frac{1}{\tau^{3/2}} \frac{1}{\sqrt{D_c}} \left[\frac{1}{(\gamma_0-1)^2}(1-x)\right.$$
$$\left. - e^{-x^2/4D_c\tau\mu^2}\left(\frac{1}{(\gamma_0-1)^2} + \frac{1}{\gamma_0-1}z\right)\right].$$

Note the singular behavior of solution (17) for temperature at $(x=0, \tau=0)$ through the behavior of the exponential term multiplied by $1/\sqrt{\tau}$, which tends to $1 - \delta(x)$ when time tends to zero.

For density, the asymptotic behaviors obtained from Eqs. (14) and (15) are

$$\rho_{BL}^{PE} \approx 1 - \frac{\alpha}{\mu} \frac{2}{3} \frac{1}{(\gamma_0-1)} \frac{1}{\sqrt{D_c}} \frac{1}{\sqrt{\pi}} e^{-z^2/4D_c\tau},$$
(18)
$$\rho_B^{PE} \approx 1 + \alpha \frac{2}{3} \frac{1}{\gamma_0-1} \left(1 - \frac{1}{(\gamma_0-1)} \frac{1}{\sqrt{\pi}\sqrt{D_c}\sqrt{\tau}}\right).$$

The matching condition between density in the bulk and density in the boundary layer is fulfilled on the piston effect time scale, that is to say, when $\tau = O(1)$. The equation

$$\lim_{x \to \infty}(\rho_{BL}^{PE}-1) = O\left(\frac{\alpha}{\mu}\right) \times 0$$
(19)

means that the density in the boundary layer matches the density in the bulk since the first perturbation in the bulk from Eq. (18) is of order α, that is to say, much smaller than α/μ. However, it is clear from the above equations (18) that, when time tends to infinity, density in the bulk phase tends to a constant of order of magnitude α. As density in the boundary layer continues to decrease with time, it becomes of an order of magnitude such that the matching condition written above [Eq. (19)] is no longer valid since

$$\lim_{\tau \to \infty}\lim_{z \to \infty}(\rho_{BL}^{PE}-1) = \alpha \times 0$$

$$\neq \alpha \times \frac{2}{3} \frac{1}{\gamma_0-1}$$

$$= \lim_{\tau \to \infty}\lim_{x \to 0}(\rho_B^{Pe}-1).$$
(20)

It is thus necessary to introduce a new time scale such that density is of the same order of magnitude throughout the whole domain. If $\theta = \xi\tau$ is such a time scale, longer than the τ scale ($\xi \ll 1$), it should be such that density in the bulk and density in the boundary layer are of the same order of magnitude to fulfill the matching between the two domains. ξ is thus such that

$$\frac{\alpha}{\mu}\sqrt{\xi} = \alpha \Rightarrow \xi = \mu^2.$$

Density relaxation thus occurs on a time scale θ defined by

$$\theta = \mu^2\tau = \varepsilon\sqrt{\mu}t,$$
(21)

which shows that the θ scale, which is $\sqrt{\mu}$ longer than the heat diffusion scale in the perfect gas (εt), is nothing other than the divergently long heat diffusion time in the supercritical fluid. This time scale will drive the system to complete thermodynamic equilibrium. Without entering further into the detailed solution of the equations that describe the density relaxation, we should comment on some consequences of the introduction of this heat diffusion time scale.

It can first easily be checked that rewriting expressions (18) as a function of the time variable θ by using Eq. (21) makes the boundary layer disappear since diffusion is observed now on the diffusion time scale:

$$\rho_{BL}^{PE} \approx 1 - \frac{\alpha}{\mu} \frac{2}{3} \frac{1}{(\gamma_0-1)\sqrt{D_c}} \frac{1}{\sqrt{\pi}\sqrt{\tau}} e^{-z^2/4D_c\tau}$$

$$= 1 - \alpha \frac{2}{3} \frac{1}{(\gamma_0-1)\sqrt{D_c}} \frac{1}{\sqrt{\pi}\sqrt{\theta}} e^{-x^2/4D_c\theta},$$

$$\rho_B^{PE} \approx 1 + \alpha \frac{2}{3} \frac{1}{\gamma_0-1}\left(1 - \frac{1}{(\gamma-1)\sqrt{\pi}\sqrt{D_c}} \frac{1}{\sqrt{\tau}}\right)$$

$$= 1 + \alpha \frac{2}{3} \frac{1}{(\gamma_0-1)} + O(\alpha\mu).$$

The matching conditions can be written formally as

$$\lim_{\tau \to \infty} X(x,\tau) = \lim_{\theta \to 0} X(x,\theta)$$

for all dependent variables, so one must consider that Eqs. (17) and (18) written in terms of θ are the initial conditions for the equations describing the evolution on the θ scale. These initial conditions, although singular for $\theta=0$, show that the temperature perturbations in the cell decrease on the τ scale from their initial order of magnitude α to the order of magnitude $\alpha\mu$, which is hardly accessible to experiments.

Similarly, the asymptotic behavior for density indicates that the density perturbation decreases on the τ scale from the order of magnitude α/μ to the order α. α is the order of magnitude of the density perturbation at the end of the heating period if the gas is an ideal one or set very far away from its critical conditions in the one-phase region. This means that this period is accessible to experiments, but the singular behavior should be overcome if a valid description of the density relaxation is to be used.

B. Description of density relaxation on the θ scale

When rewritten as a function of the variable θ, the expansions of the hydrodynamic variables for $\tau \to \infty$ as given by Eqs. (17) and (18) become

$$p \approx \frac{3}{2}(1+\mu) - \frac{9}{8} + \alpha\frac{3}{2} - \alpha\mu\frac{3}{2}\frac{1}{\gamma_0 - 1}\frac{1}{\sqrt{\pi}}\frac{1}{\sqrt{D_c}\sqrt{\theta}},$$

$$T \approx 1 + \alpha - \alpha\mu\frac{1}{\sqrt{\pi}\sqrt{D_c}}\frac{1}{\gamma_0 - 1}\frac{1}{\sqrt{\theta}}(1 - e^{-x^2/4D_c\theta}),$$

$$(22)$$

$$u \approx -\alpha\varepsilon\sqrt{\mu}\frac{1}{3}\frac{1}{\sqrt{\pi}\sqrt{D_c}}\frac{1}{\gamma_0 - 1}\frac{1}{\theta^{3/2}}xe^{-x^2/4D_c\theta},$$

$$\rho \approx 1 - \alpha\frac{2}{3}\frac{1}{\gamma_0 - 1}\left(\frac{1}{\sqrt{\pi}\sqrt{D_c}}\frac{1}{\sqrt{\theta}}e^{-x^2/4D_c\theta} - 1\right).$$

According to the matching principle, which imposes for p, T, u, and ρ

$$\lim_{\tau\to\infty} X(x,\tau) = \lim_{\theta\to 0} X(x,\theta),$$

Eqs. (22) give the initial conditions for evolution on the θ scale. They are the legacy of the piston effect on the diffusion scale: a strong depletion in the heated wall region and a homogeneous overdensity in the bulk region. They are also singular, i.e., they can be written as generalized functions. The one for ρ is, for example,

$$\lim_{\theta\to 0} \rho(x,\theta) = -\frac{2}{3}\frac{1}{\gamma_0 - 1}[\delta(x) - 1].$$

Equations (22) also indicate that the solutions that describe the evolution of the legacy of the piston effect on the θ scale must be sought under the form of the following asymptotic expansions:

$$T^p(x,\theta) \approx 1 + \mu + \alpha H_{[0]}(\theta) + \alpha\mu\tilde{T}(x,\theta),$$

$$p^p(x,\theta) \approx \tfrac{3}{2}(1+\mu) - \tfrac{9}{8} + \tfrac{3}{2}\alpha H_{[0]}(\theta) + \alpha\mu\tilde{p}(x,\theta),$$

$$\rho^p(x,\theta) \approx 1 + \alpha\tilde{\rho}(x,\theta),$$

$$u^p(x,\theta) \approx \alpha\varepsilon\sqrt{\mu}\,\tilde{u}(x,\theta). \tag{23}$$

Carrying these expansions into the Navier-Stokes equations leads to the following system of equations:

$$\frac{\partial\tilde{\rho}}{\partial\theta} + \frac{\partial\tilde{u}}{\partial x} = 0,$$

$$\frac{\partial\tilde{p}}{\partial x} = 0,$$

$$(24)$$

$$\frac{3}{2}\frac{\partial\tilde{u}}{\partial x} - D_c\frac{\partial^2\tilde{T}}{\partial x^2} = \frac{t_0}{\gamma - 1}\delta(\theta),$$

$$\tilde{p} = \tfrac{3}{2}\tilde{T} + \tfrac{9}{4}\tilde{\rho},$$

which must be complemented by singular initial conditions given by the limits for $\theta \to 0$ of expressions (22), and by the following boundary conditions:

$$\tilde{T} = 0, \quad \tilde{u} = 0 \quad \text{at } x = 0,$$

$$\frac{\partial\tilde{T}}{\partial x} = 0, \quad \tilde{u} = 0 \quad \text{at } x = 1.$$

It must be emphasized here that the energy equation in Eqs. (24) involves both the compression term of pressure forces and the diffusion term. The hypercompressibility property thus influences the bulk equations even though, on earlier time scales, it acts on the bulk only through boundary matching, i.e., there is a strong mass addition in the bulk but unchanged acoustic equations compared to the ideal gas. This is a consequence of the fact that, at earlier times, the bulk process is governed by acoustic isentropic modes only and thus by the isentropic compressibility, which does not show a dramatic singular behavior. On the diffusion time scale, the bulk phase no longer undergoes an isentropic process and the isothermal compressibility acts on the bulk phase as it did in the boundary layer only on shorter time scales. The system of equations (24) is solved by means of the Laplace transform and only needs the use of classical transform tables. Details are given in the Appendix. However, we can already see that density is driven by a pure diffusion equation, which is striking for a pure fluid:

$$\frac{\partial\rho}{\partial\theta} - D_c\frac{\partial^2\rho}{\partial x^2} = \frac{2}{3}\frac{1}{\gamma - 1}\delta(\theta).$$

The solution obtained for the hydrothermodynamic variable can be written as follows on the θ scale:
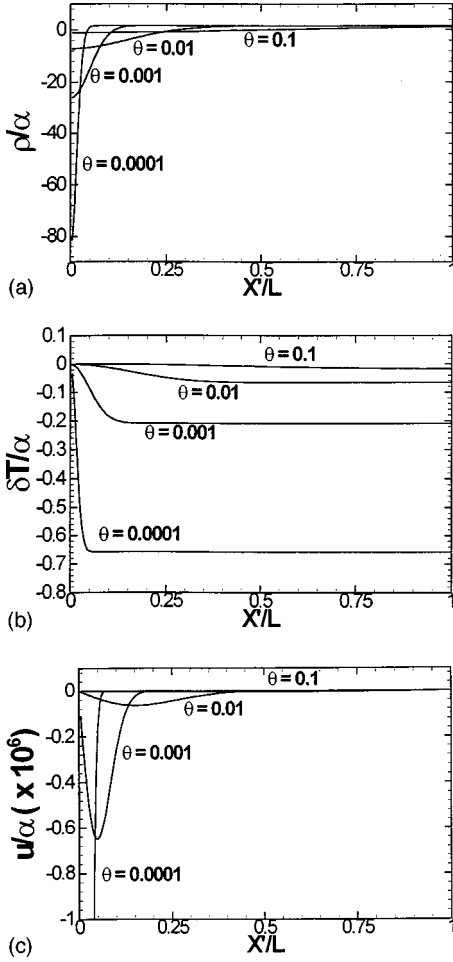
FIG. 1. Evolution of hydrodynamic variables within the sample as given by the solution valid on the heat diffusion time scale: (a) density, (b) temperature, and (c) velocity.

$$\tilde{T}(x,\theta) = 2\frac{1}{\gamma_0-1}\sum_{n=1}^{\infty}\exp(-n^2\pi^2 D_c\theta)$$
$$\times(-1+(-1)^n\{\cos[n\pi(1-x)]\}),$$

$$\tilde{p}(x,\theta) = \frac{3}{2}\frac{1}{\gamma_0-1}\left(1-2\sum_{n=1}^{\infty}\exp(-n^2\pi^2 D_c\theta)\right),$$

(25)

$$\tilde{\rho}(x,\theta) = \frac{2}{3}\frac{1}{\gamma_0-1}\left(1-2\sum_{n=1}^{\infty}(-1)^n\right.$$
$$\left.\times\exp(-n^2\pi^2 D_c\theta)\cos[n\pi(1-x)]\right),$$

$$\tilde{u}(x,\theta) = \frac{2}{3}\frac{1}{\gamma_0-1}\left((1-x)\delta(\theta)-2\pi D_c\right.$$
$$\left.\times\sum_{n=1}^{\infty}\exp(-n^2\pi^2 D_c\theta)(-1)^n\sin[n\pi(1-x)]\right).$$

The functions $\tilde{p}$, $\tilde{\rho}$, $\tilde{T}$, and $\tilde{u}$ that are plotted on Figs. 1(a)–1(c) show clearly the singular behavior of the solution for the θ scale when $\theta\to 0$, which can be removed by applying the additive composition matching procedure to the solutions on the θ and τ time scales. This shows that density relaxation on the long time scale is that of an initial Dirac-like strong mass depletion at $x=0$ in a medium initially not at equilibrium. This configuration is the remains of the temperature inhomogeneities left by the piston effect, which diffuse to complete equilibrium on the long diffusion time scale. These functions can be checked to smoothly match with expansions (17) and (18) when $\theta\to 0$.

C. Uniformly valid description for boundary heating: The whole field

In the preceding sections, three characteristic times have been mentioned: the acoustic time scale, the piston effect time scale, and the heat diffusion time scale. The acoustic time scale does not intervene directly in experiments on temperature or density relaxation, so we shall focus our attention on the piston effect time scale and the heat diffusion time scale only. The additive composition procedure is used to obtain a uniform description in time from the initial heating to complete equilibrium. If X denotes u,p,T, or ρ, then the additive composition procedure consists of constructing the following function that is uniformly valid at any time scale:

$$X(x,\theta) = X^{\text{PE}}\left(x,\tau=\frac{\theta}{\mu^2}\right) + X^\rho(x,\theta)$$
$$-\begin{cases}\lim_{\theta\to 0}X^\rho(x,\theta)\\ \lim_{\theta/\mu^2\to\infty,\,\theta\ll 1}X^{\text{PE}}(x,\tau).\end{cases}$$

(26)

Both limits in this formula are, of course, equal because matching was imposed between the descriptions obtained on different time scales. The τ scale (piston effect) appears to be an initial boundary layer in time for the heat diffusion time scale: temperature relaxation by the piston effect occurs within an initial boundary layer in time, the thickness of which is μ^2, i.e.,

$$\tau = \frac{\theta}{\mu^2}.$$

In a similar way, the uniformly valid description in space has been written as a function of the largest space scale x. The uniformly valid description in time is expressed here as a function of time counted on the largest scale in time (the heat diffusion time). The analytical expressions for the hydrodynamic variables that are valid over all the length and time scales are thus

$$T(x,\theta)=1+\mu+\alpha\left[1-e^{(\gamma_0-1)^2 D_c\theta/\mu^2}i^0\mathrm{erfc}\left((\gamma_0-1)\sqrt{D_c}\frac{\sqrt{\theta}}{\mu}\right)+e^{[(\gamma_0-1)x/\mu+(\gamma_0-1)^2\sqrt{D_c}\sqrt{\theta}/\mu]}\right.$$

$$\times i^0\mathrm{erfc}\left((\gamma_0-1)\sqrt{D_c}\frac{\sqrt{\theta}}{\mu}+\frac{x}{2\sqrt{D_c}\sqrt{\theta}}\right)\Bigg]+\alpha\mu\frac{1}{(\gamma_0-1)\sqrt{D_c}}\left(2\sqrt{D_c}\sum_{n=1}^{\infty}e^{-n^2\pi^2 D_c\theta}\{-1+(-1)^n\right.$$

$$\left.\times\cos[n\pi(1-x)]\}+\frac{1}{\sqrt{\pi}}\frac{1}{\sqrt{\theta}}(1-e^{-x^2/4D_c\theta})\right),$$

$$\rho(x,\theta)=1-\frac{2}{3}\frac{\alpha}{\mu}e^{[D_c(\gamma_0-1)^2\theta/\mu^2+(\gamma-1)x/\mu]}i^0\,\mathrm{erfc}((\gamma_0-1)\sqrt{D_c}\sqrt{\theta}/\mu)i^0\,\mathrm{erfc}\left((\gamma_0-1)\sqrt{D_c}\sqrt{\theta}/\mu+\frac{x/\mu}{2\sqrt{D_c}\sqrt{\theta}/\mu}\right)$$

$$+\alpha\frac{2}{3}\{1-e^{(\gamma_0-1)^2 D_c\theta/\mu}i^0\,\mathrm{erfc}[(\gamma_0-1)\sqrt{D_c}\sqrt{\theta}/\mu]\}+\alpha\frac{2}{3}\frac{1}{\sqrt{D_c}(\gamma_0-1)}\left(\frac{e^{-x^2/4D_c\theta}}{\sqrt{\pi}\sqrt{\theta}}\right.$$

$$\left.-\sqrt{D_c}2\sum_{n=1}^{\infty}(-1)^n e^{-n^2\pi^2 D_c\theta}\cos[n\pi(1-x)]\right).$$

(27)

$$u(x,\theta)=\frac{\alpha\varepsilon}{\mu^{3/2}}\frac{2}{3}\sqrt{D_c}\left\{(1-x)\left[\frac{1}{\sqrt{\pi}\sqrt{\theta/\mu}}-(\gamma_0-1)\sqrt{D_c}e^{(\gamma_0-1)^2 D_c\theta/\mu^2}\mathrm{erfc}\left((\gamma_0-1)\sqrt{D_c}\frac{\sqrt{\theta}}{\mu}\right)\right]-\frac{e^{-(x^2/\mu^2)/4D_c\tau}}{\sqrt{\pi}\sqrt{\theta/\mu}}\right.$$

$$\left.+(\gamma_0-1)\sqrt{D_c}e^{(\gamma_0-1)^2 D_c\theta/\mu^2+(\gamma_0-1)x/\mu}\mathrm{erfc}\left((\gamma_0-1)\sqrt{D_c}\sqrt{\theta}/\mu+\frac{x}{2\sqrt{D_c}\sqrt{\theta}}\right)\right\}$$

$$+\alpha\varepsilon\sqrt{\mu}\frac{2}{3}\frac{1}{\gamma_0-1}\left(\frac{xe^{-x^2/4D_c\theta}}{2\sqrt{D_c}\sqrt{\pi}\sqrt{\theta^3}}-2\pi D_c\sum_{n=1}^{\infty}e^{-n^2\pi^2 D_c\theta}(-1)^n\sin[n\pi(1-x)]\right),$$

$$p(x,\theta)=\tfrac{3}{2}(1+\mu)-\tfrac{9}{8}+\alpha\frac{3}{2}\left[1-e^{(\gamma_0-1)^2 D_c\theta/\mu^2}i^0\,\mathrm{erfc}\left((\gamma_0-1)\sqrt{D_c}\frac{\sqrt{\theta}}{\mu}\right)\right]+\alpha\mu\frac{3}{2}\frac{1}{\gamma_0-1}\left(\frac{1}{\sqrt{\mu}\sqrt{D_c}\sqrt{\theta}}-2\sum_{n=1}^{\infty}e^{-n^2 n^2 D_c\theta}\right).$$

The pressure being homogeneous for all times, there is only an initial boundary layer.

V. RESULTS AND DISCUSSION

A. Typical values for the parameters

In what follows we consider parameters that correspond to experimental conditions not very close to the critical point, but the parameter μ can be changed if necessary. The parameters used are sample cell 10^{-2} m in length, and sample fluid, carbon dioxide:

$$\kappa_0'=3.25\times10^{-8}\ \mathrm{m^2\,s^{-1}};\quad \nu'=7.3\times10^{-8}\ \mathrm{m^2\,s^{-1}};$$

$$\rho_c'=467.8\ \mathrm{kg\,m^{-3}};\quad T_c'=304.13\ \mathrm{K}.$$

The initial conditions are

$$T'=T_c'+1.5\ \mathrm{K};\quad \rho'=\rho_c',$$

and the corresponding parameters

$$D_c=1.15,\quad Pr=2.274,\quad \varepsilon=2.274\times10^{-8},\quad \mu=5\times10^{-3}.$$

The heating function used is a boundary temperature increase of $\Delta T'=0.02$ K in $\Delta t'=0.1$ s, that is to say, $\alpha=6.6\times10^{-5}$, $t_0=2.8\times10^3$. The heating is thus over very early on the piston effect time scale, which is defined by Eq. (13), since the piston characteristic time is of the order of 0.442 s, which has to be compared to 0.1 s of heating time. The characteristic time for heat diffusion in a critical fluid set in the initial conditions described above is equal to $16\,700$ s (calculated as L^2/κ') whereas it is 3076 s (calculated as L^2/κ_0') in the ideal gas.

B. Orders of magnitude

1. Time regions

The orders of magnitude of the time periods that have been pointed out compare well with the one found by Onuki and Ferrel [10], the slight differences coming from the fact that the definition of orders of magnitude may differ from one approach to the other. We shall give the name ''piston effect period'' to values of time such that

$$0<\frac{\theta}{\mu^2}\leqslant1.$$

The matching with the acoustic period could also have been performed on the basis of the available solutions on the different time scales but this would not have provided new insights into density relaxation.

After the piston effect period comes the overlapping period of time, or intermediate period, which corresponds mathematically to the matching zone between the solutions that describe the evolution on the τ scale (piston effect) and on the θ scale (diffusion). This period is defined by values of time θ such that

$$\frac{\theta}{\mu^2} \gg 1 \quad \text{and} \quad \theta \ll 1.$$

Depending on the location, this period of time is centered on different values of time but the above asymptotic relation is always fulfilled.

After the overlapping period is over, the long diffusion period starts, which is simply defined by

$$\theta = O(1).$$

2. Orders of magnitude of the dependent variables

The orders of magnitude of the different dependent variables as they vary on the different time scales can be discussed. We shall comment particularly on density and temperature. It should be recalled first that, due to the diverging isothermal compressibility, the order of magnitude of the density perturbation is greater than that of the temperature perturbation by a factor μ. During the piston effect time scale, after the wall heating has been stopped, the temperature inhomogeneity is of order α, while the density inhomogeneity is still of order α/μ. At the end of the piston effect period (0.44 s under the present conditions), as shown by Eq. (22), temperature is homogenized at order $\alpha \mu$ while the density inhomogeneity has relaxed to the order of magnitude α it would have if the fluid were an ideal gas. Then, in the heat diffusion period (referred to a unit time of 4 h and 37 min under the presently chosen typical conditions), temperature and density inhomogeneities relax diffusively to complete equilibrium. This means that the heat diffusion period, which evens out the very small temperature inhomogeneities left by the piston effect, involves hardly measurable temperature differences. To a first approximation the piston effect relaxes temperature first while heat diffusion relaxes density later on. Density and temperature thus reach a given small value considered as a relaxed value on different time scales and by different mechanisms. This is why one can illustrate this feature by saying that the two relaxation processes are uncoupled in near-critical fluids. Of course, the variables themselves are still coupled but differently from the way they are in ideal gases. This is indeed the case when one looks at the approximate equation of state in the nondissipative regions (the bulk phase on the acoustic or piston effect time scales). It can be written as follows [16,20]:

$$\nu \, \delta P = \alpha \, \delta T,$$

which means that there is a real uncoupling of temperature and density in the equation of state that is specific to near-critical fluids. The driving force for the evolution in bulk
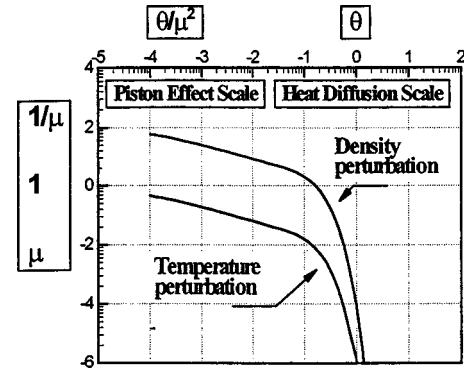

FIG. 2. Evolution of temperature (solid) and density (dashed) perturbation in the sample cell.

phases during the piston effect period is an acoustic field generated by mass addition from the expanding boundary-layer region. As temperature and density perturbations in an acoustic field have the same order of magnitude, the density perturbation term in the equation of state, which is multiplied by the reciprocal of the isothermal compressibility, is negligible compared to the pressure and temperature terms. Density and temperature in nondissipative regions are coupled only through velocity and the mass conservation statement. On the diffusion time scale, when diffusion fills the whole bulk phase, heat diffusion is again the driving force in the same way it was the driving force on earlier time scales in the boundary layers. So density and temperature perturbation have huge differences in orders of magnitude and are thus directly coupled in the equation of state.

C. Evolution of density and temperature inhomogeneities in a near-critical 1D sample from the initial heat deposit to complete equilibrium

Both temperature and relaxation effects are simultaneously present but they intervene at different orders of magnitude in a given time frame. The evolutions of the normalized density and temperature inhomogeneities within the sample are defined by

$$\Delta\rho = \frac{\rho(1,\theta) - |\rho(0,\theta)|}{\alpha} \quad \text{and} \quad \Delta T = \frac{1 + \mu + \varepsilon t_0 - T(1,\theta)}{\alpha}$$

and plotted on Fig. 2 on a log-log scale as a function of time counted in units of the heat diffusion time.

The normalized inhomogeneity would be of order 1 in an ideal gas. It is clear first that density and temperature always keep a ratio μ because of the diverging compressibility. In the time period when solutions on both the piston effect time scale and the diffusion time scale are simultaneously valid, the time variable satisfying the condition

$$\frac{\theta}{\mu^2} \gg 1 \quad \text{and} \quad \theta \ll 1,$$

which can be considered to extend from $\theta = 2.5 \times 10^{-5}$ to $\theta = 2.5 \times 10^{-1}$, the density perturbations become of order 1, which means that they take the value they would have if the fluid were an ideal gas or at least a normally compressible one. At the same time, temperature has reached the order of
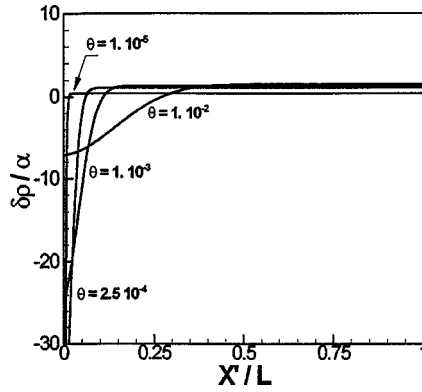
FIG. 3. Density perturbation in the sample as given by the uniformly valid solution.

FIG. 4. Velocity in the sample as given by the uniformly valid description.

magnitude $\alpha\mu$, which can be considered as the new equilibrium at first order. In that time frame, density and temperature follow the matching function in time of Eq. (17) written at $x=0$ and thus keep decreasing as $1/\sqrt{\theta}$, which was mentioned as the bulk behavior by Onuki and Ferrel [10]. We shall see later that the present theory leads to a different behavior in the bulk. For larger values of θ, the density inhomogeneity undergoes exponential decay as also predicted by Onuki and Ferrel [10] and detected as a ''long diffusive tail'' in the experiments by Boukari, Pego, and Gammon [12]. This diffusive decay thus occurs in an isothermal medium at first order.

D. Density profiles within the 1D sample

The density profiles are plotted on Fig. 3 for different times from the late piston effect period ($\theta=2.5\times10^{-5}$) to the early diffusion time scale ($\theta=10^{-2}$). These values of time cover the intermediate period. The deeply depleted area located near the heated wall for small values of θ corresponds to the thermal boundary layer that lost mass during the piston effect period. As time increases, the diffusion depth is wider and back-diffusion begins to fill the depleted boundary-layer area again. It should be noted that the bulk region continues to be compressed because density in the bulk keeps increasing in time. This specific behavior is demonstrated by the uniformly valid description that accounts for both the piston effect and bulk diffusion in the intermediate period of time. This means that at the same time as diffusion begins driving the system back to equilibrium in the boundary-layer area, the piston effect keeps driving the system out of equilibrium by compressing the bulk phase. It can be checked in Fig. 2 that the bulk density instead decreases monotonically in time when described by the solution valid in the heat diffusion time period only. The velocity plots for the same values of time as the density profiles (Fig. 4) show that a return flow (negative velocity) appears in the boundary layer region while the velocity is still positive in the bulk, which confirms that there is still mass addition and thus a piston effect. Accordingly, there is an inversion of the velocity gradient in the sample which will be shown, in the next section, to play an important role in the relaxation process. For larger values of time, when one enters the diffusion period, the diffusion area reaches a macroscopic scale in the
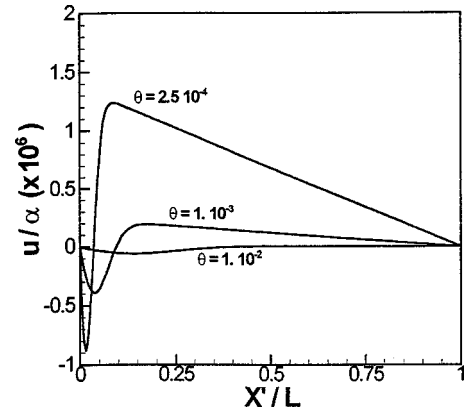
sample, the velocity is negative everywhere, there is no longer a piston effect, and diffusion becomes the only driving force.

E. Time history of density at different locations in the sample

In this section we explore the evolution of density over time at different locations in the sample by studying the normalized density perturbation as defined by

$$\Delta\rho = \frac{\rho(x,\theta)-1}{\alpha}.$$

Even if some locations are below the resolution in space that it is possible to achieve in real experiments, we shall present them to back up the coherence of the whole theory. As the piston effect time scale appears as a boundary layer in time, the results are presented in a log-Cartesian frame. The different features concerning the density time history at a given location will be correlated in the next section with those concerning the velocity field.

1. Time history of density at a point located in the middle of the bulk ($x=0.5$)

Figure 5 represents the time history and shows that, on the piston effect period, density increases according to the mass
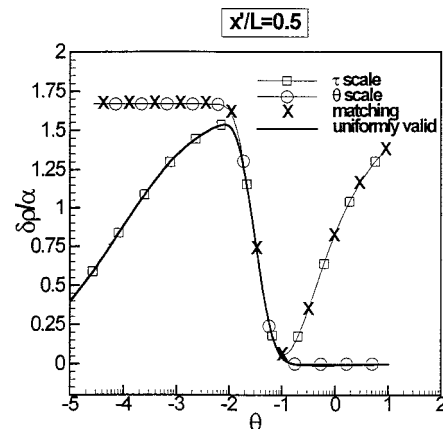

FIG. 5. Evolution of density at $x=0.5$ as given by the uniformly valid description and plotted as a function of the time in units of heat diffusion characteristic time.
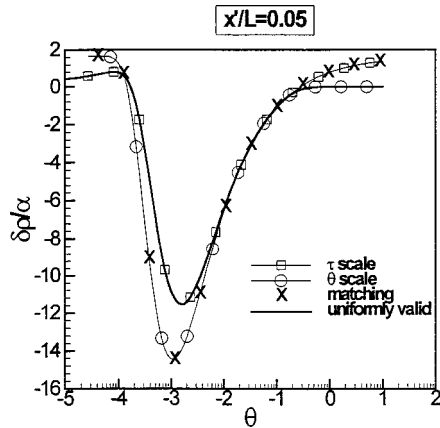
FIG. 6. Evolution of density at $x=0.1$ as given by the uniformly valid description and plotted as a function of the time in units of heat diffusion characteristic time.

FIG. 7. Evolution of the density at $x=0.01$ as given by the uniformly valid description and plotted as a function of the time in units of heat diffusion characteristic time.

transfer from the boundary-layer region to the bulk. Then, in the intermediate period, the density drops down suddenly because the piston effect ceases and the return flow refills the depleted area near the origin. The density drop follows the matching function given by Eq. (22) for ρ. This function has also been plotted in Fig. 5 with the solutions that are valid on the τ scale (piston effect) and on the θ scale (diffusion) to illustrate the concept of asymptotic matching and make things clearer. In particular, it is visible without further demonstration that the common part of the three functions is the increasing branch of the matching function

$$\frac{1}{\sqrt{\pi}} \frac{1}{\sqrt{D_c}\sqrt{\theta}} e^{-x^2/4D_c\theta} - 1$$

given by Eq. (22) at $x=0.5$. One can thus say that, when the thermal boundary layer passes a given location within the bulk, it can be detected by a steep decrease to the initial equilibrium as $(1/\sqrt{\theta})e^{-x^2/4D_c\theta}$. For larger values of time referred to the diffusion time (θ), the density continues to relax monotonically. This part of the curve, which extends approximately from $\theta=1$ to infinity, represents the long exponential diffusive tail that drives the system back to equilibrium. One should remember here that the characteristic time is 4 h and 37 min. This shows that the intermediate region plays an important role in the density relaxation process.

2. Time history at points located close to the heated boundary

The time histories of density at two measurement stations located at $x=5\times10^{-2}$ and 0.1 as given by our analytic solution are plotted in Figs. 6 and 7, respectively, in the same system of coordinates as in Fig. 5. The evolution at these locations, in contrast with that in the bulk, is no longer monotonic. Density still experiences an increase first because the piston effect still has time to increase it by isentropic compression before the diffusion layer extends to the location. The increasing period is longer when the location is farther from the boundary since it takes a longer time for diffusion to reach it. Then, as time goes by, heat diffusion reaches the location under consideration (of course much earlier than in the bulk) and density thus decreases strongly,
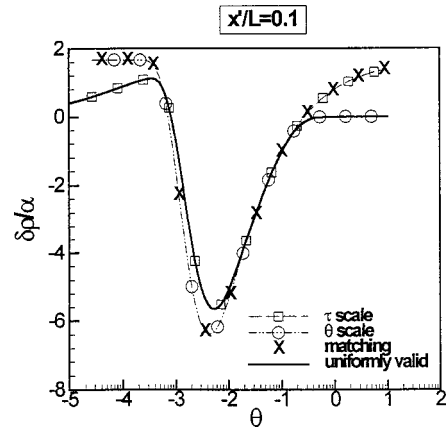
even to negative values, since this station now belongs to the thermal boundary layer. Continuation of the evolution for longer times displays another difference from that in the bulk: when the return flow appears, density again increases diffusively by following the long diffusive exponential tail to reach the final equilibrium value again.

3. Time history at the heated wall

At the heated wall, as plotted in Fig. 8, density increases monotonically in absolute value since it belongs to the thermal boundary layer at all times and thus never experiences the piston effect.

F. Density and velocity in the sample: An expansion-compression zone traveling at the diffusion velocity

The preceding section can be summarized in the following way: density only increases monotonically in time at the heated boundary (in fact it decreases first during the heating period, which is not visible on the heat diffusion time scale); it increases, decreases, and increases again in time when close to the heated boundary; it only increases and decreases in time when far in the bulk. In order to obtain a better
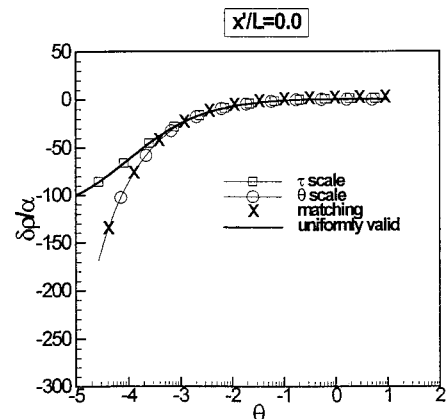

FIG. 8. Evolution of the density at $x=0$ as given by the uniformly valid description and plotted as a function of the time in units of heat diffusion characteristic time.
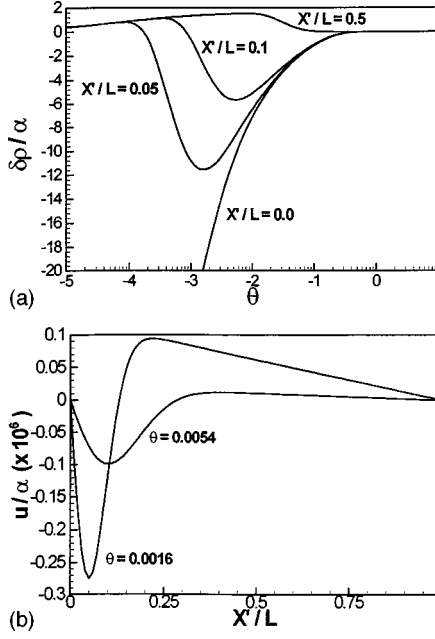
FIG. 9. Evolution of density and velocity. (a) Density as a function of time at various locations in the sample; (b) velocity profile in the sample at the moment when density is minimum at the location under consideration.

understanding of the processes involved, we must correlate the density field with the hydrodynamic velocity field in the sample.

From Eqs. (27), which give the uniformly valid descriptions, we plot in Fig. 9(a) the time histories at some locations, among which are those mentioned in the preceding section. When measurement stations farther from the heated wall are considered, the minimum is less and less pronounced and disappears completely, giving way to a simple decay to the initial equilibrium. We also plot in Fig. 9(b) the velocity profiles within the sample at the moment when density is minimum. For the measurement stations at $x = 0.05$ and 0.1, the velocity profile in the sample exhibits a minimum located at the measurement station under consideration. For values of x greater than the given location, the velocity gradient is positive, corresponding to an expansion zone, while for smaller values of x the velocity gradient is negative, corresponding to a compression region. The density variation in time at a given location is thus the result of the passage of an expansion-compression zone traveling rightward at the diffusion speed, the driving force of which is the diffusion of a given initial density perturbation in a nonequilibrium homogeneous hypercompressible medium. Density first drops since the fluid is accelerated to the left; then, as the expansion-compression zone propagates rightward, a compression occurs since the velocity must be zero at the left boundary and density increases again. While traveling rightward, the depth of the velocity minimum decreases, eventually to disappear completely. In fact, the low-density zone created at the heated wall is filled, while moving rightward, by the bulk density excess. It ultimately disappears before reaching the other end of the sample cell.

This is why, for the measurement station located at $x = 0.5$, the evolution is again a monotonic relaxation, since the compression branch of the velocity profile has disap-

peared, in the same way as it loses its expansion branch very close to the wall. The point beyond which the density history becomes a simple relaxation in the bulk phase is given by the location where the minimum in the velocity profile disappears. This means that, beyond this particular location, the bulk never experiences the initial diffusion boundary layer but only the leftward diffusion that drives the bulk back to thermodynamic equilibrium.

VI. GENERALIZATION TO REAL CRITICAL EXPONENTS

As the sound velocity tends to zero when the critical point is approached in the supercritical region on the critical isochore, accounting for the variations of the specific heat at constant volume requires a definition of nondimensional time as follows:

$$t = \frac{t'}{t'_a}, \quad t'_a = L' / \sqrt{\gamma_0 r' T'_c} \sqrt{C'_\nu / C'_{\nu 0}},$$

where $C'_{\nu 0}$ is the specific heat at constant volume far from the critical point. The nondimensional equations of continuity, momentum, and energy can be written as

$$\sqrt{C'_{\nu 0} / C_\nu} \rho_t + (\rho u)_x = 0,$$

$$\sqrt{C'_{\nu 0} / C'_\nu} \, \rho u_t + \rho u u_x = -\frac{1}{\gamma_0} P_x + \tfrac{4}{3} \varepsilon u_{xx},$$

$$\sqrt{C'_\nu / C'_{\nu 0}} (\rho T_t + \rho u T_x) = -(\gamma_0 - 1) T \left(\frac{\partial P}{\partial T} \right)_\rho u_x$$
$$+ \varepsilon \left\{ \frac{\gamma_0}{Pr_0} \left[\left(\frac{\lambda'}{\lambda'_0} \right) T_{xx} + \left(\frac{\lambda'}{\lambda'_0} \right)_x T_x \right] \right\}$$
$$+ \frac{4}{3} \varepsilon \gamma_0 (\gamma_0 - 1) u_x^2.$$

The equation of state is written in its linearized form as

$$P - P_i = \left(\frac{\partial P}{\partial T} \right)_{\rho} \bigg|_{T_i, \rho_i} (T - T_i) + \left(\frac{\partial P}{\partial \rho} \right)_T \bigg|_{T_i, \rho_i} (\rho - \rho_i),$$

where the subscript i denotes the initial conditions. The critical behaviors are given by

$$\sqrt{C'_\nu / C'_{\nu 0}} \simeq \mu^{-\alpha}, \quad \left(\frac{\partial P}{\partial \rho} \right)_T \simeq \mu^\gamma, \quad \left(\frac{\lambda'}{\lambda'_0} \right) = \mu^{-c}.$$

In order to avoid misunderstanding, the order of magnitude of the temperature increase at the boundary is denoted by φ in this section.

Similar arguments to those used for the van der Waals gas analysis lead to the following definitions of the time scales:

$$\tau = \varepsilon \left(\frac{3\rho}{\partial P} \right)_T \left(\frac{\lambda'}{\lambda'_0} \right) (\sqrt{C'_{\nu 0} / C'_\nu})^{3/2} t$$

for the piston effect time scale τ and

$$\theta = \left(\frac{C'_\nu}{C'_{\nu 0}}\right)^2 \left(\frac{\partial P}{\partial \rho}\right)_T^2 \tau$$

for the density relaxation time scale θ. When expressed as a function of the critical components, the above relations become

$$\tau = \varepsilon \mu^{-\gamma - c + 3\alpha/2} t \quad \text{and} \quad \theta = \mu^{2\gamma - 2\alpha} \tau.$$

The boundary-layer thickness is found to be $\delta = (\partial P/\partial\rho)_T(C'_\nu/C'_{\nu 0})$ on the piston effect time scale, or $\delta = \mu^{\gamma - \alpha}$ when expressed as a function of the critical exponents.

The solutions on the piston effect and density relaxation time scales can be written as

$$T^{\mathrm{PE}} = 1 + \mu + \varphi\left[1 - e^{(\gamma_0-1)^2 D_c \tau} i^0 \,\mathrm{erfc}[(\gamma-1)\sqrt{D_c}\sqrt{\tau}] \right.$$

$$+ e^{[(\gamma_0-1)\bar{z} + (\gamma-1)^2\sqrt{D_c}\sqrt{\tau}]} i^0 \,\mathrm{erfc}\left((\gamma_0-1)\sqrt{D_c}\sqrt{\tau} \right.$$

$$\left. \left. + \frac{\bar{z}}{2\sqrt{D_c}\sqrt{\tau}} \right) \right],$$

$$\rho^{\mathrm{PE}} = 1 - \frac{\varphi}{\mu^\gamma}\frac{2}{3} e^{[D_c(\gamma_0-1)^2\tau + (\gamma-1)\bar{z}]}$$

$$\times i^0\mathrm{erfc}[(\gamma_0-1)\sqrt{D_c}\sqrt{\tau}] i^0 \,\mathrm{erfc}\left((\gamma_0-1)\sqrt{D_c}\sqrt{\tau} \right.$$

$$\left. + \frac{\bar{z}}{2\sqrt{D_c}\sqrt{\tau}} \right),$$

$$P_{\mathrm{PE}} = \tfrac{3}{2}(1+\mu) - \tfrac{9}{8} + \varphi\tfrac{3}{2}\{1 - e^{(\gamma_0-1)^2 D_c\tau}$$

$$\times i^0\mathrm{erfc}[(\gamma_0-1)\sqrt{D_c}\sqrt{\tau}]\}, \tag{28}$$

$$u^{\mathrm{PE}} = \varphi\varepsilon\mu^{-\gamma-c+\alpha}\frac{2}{3}\sqrt{D_c}\left[(1-x)\left(\frac{1}{\sqrt{\pi}\sqrt{\tau}} \right.\right.$$

$$\left. - (\gamma_0-1)\sqrt{D_c}e^{(\gamma-1)^2 D_c\tau}\mathrm{erfc}[(\gamma_0-1)\sqrt{D_c}\sqrt{\tau}] \right)$$

$$- \frac{e^{-x^2/\mu^2/4D_c\tau}}{\sqrt{\pi}\sqrt{\tau}} + (\gamma_0-1)\sqrt{D_c}$$

$$\times e^{(\gamma_0-1)^2 D_c\tau + (\gamma_0-1)x/\mu}\mathrm{erfc}\left((\gamma_0-1)\sqrt{D_c}\sqrt{\tau} \right.$$

$$\left.\left. + \frac{x/\mu}{2\sqrt{D_c}\sqrt{\tau}} \right) \right],$$

whereas they are written on the density relaxation time scale as

$$T^\rho(x,\theta) \approx 1 + \mu + \alpha H_{[0]}(\theta) + \varphi\mu^{-\alpha+\gamma}\widetilde{T}(x,\theta),$$

$$p^\rho(x,\theta) \approx \tfrac{3}{2}(1+\mu) - \tfrac{9}{8} + \tfrac{3}{2}\alpha H_{[0]}(\theta) + \varphi\mu^{-\alpha+\gamma}\widetilde{p}(x,\theta),$$

$$\rho^\rho(x,\theta) \approx 1 + \varphi\mu^{-\alpha}\widetilde{\rho}(x,\theta),$$

$$u^\rho(x,\theta) = \varphi\varepsilon\mu^{\gamma-c+\alpha}\widetilde{u}(x,\theta),$$

where the functions $\widetilde{T}$, $\widetilde{p}$, $\widetilde{\rho}$, and $\widetilde{u}$ are given by Eqs. (25) The introduction of real exponents thus does not change the way the functions depend on space and time but only changes the order functions. It can be checked that when α, γ, and c take their van der Waals values, i.e., $\alpha=0$, $\gamma=1$, and $c=\tfrac{1}{2}$, one again finds the expressions written in the previous sections. In the same way as for the van der Waals gas, a uniformly valid expression can be obtained, which is expressed as

$$T(x,\theta) = 1 + \mu + \varphi\left[1 - e^{(\gamma_0-1)^2 D_c\theta/\mu^{2\gamma-2\alpha}} i^0 \,\mathrm{erfc}\left((\gamma_0-1)\sqrt{D_c}\frac{\sqrt{\theta}}{\mu^{\gamma-\alpha}} \right) \right.$$

$$\left. + e^{[(\gamma_0-1)x/\mu^{\gamma-\alpha} + (\gamma_0-1)^2\sqrt{D_c}\sqrt{\theta}/\mu^{\gamma-\alpha}]} i^0 \,\mathrm{erfc}\left((\gamma_0-1)\sqrt{D_c}\frac{\sqrt{\theta}}{\mu^{\gamma-\alpha}} + \frac{x}{2\sqrt{D_c}\sqrt{\theta}} \right) \right]$$

$$+ \varphi\mu^{-\alpha+\gamma}\frac{1}{(\gamma_0-1)\sqrt{D_c}}\left[2\sqrt{D_c}\sum_{n=1}^{\infty} e^{-n^2\pi^2 D_c\theta}\left\{ -1 + (-1)^n\cos[n\pi(1-x)] \right\} + \frac{1}{\sqrt{\pi}}\frac{1}{\sqrt{\theta}}(1 - e^{-x^2/4D_c\theta}) \right],$$

$$\rho(x,\theta) = 1 - \frac{2}{3}\frac{\varphi}{\mu^\gamma} e^{[D_c(\gamma_0-1)^2\theta/\mu^{2\gamma-2\alpha} + (\gamma_0-1)x/\mu^{\gamma-\alpha}]} i^0 \,\mathrm{erfc}[(\gamma_0-1)\sqrt{D_c}\sqrt{\theta}/\mu^{\gamma-\alpha}]$$

$$\times i^0 \,\mathrm{erfc}\left((\gamma_0-1)\sqrt{D_c}\sqrt{\theta}/\mu^{\gamma-\alpha} + \frac{x/\mu^{\gamma-\alpha}}{2\sqrt{D_c}\sqrt{\theta}/\mu^{\gamma-\alpha}} \right) + \varphi\mu^{-\alpha}\frac{2}{3}(1 - e^{(\gamma_0-1)^2 D_c\theta/\mu^{2(\gamma-\alpha)}}$$

$$\times i^0\mathrm{erfc}[(\gamma_0-1)\sqrt{D_c}\sqrt{\theta}/\mu^{\gamma-\alpha}]) + \varphi\mu^{-\alpha}\frac{2}{3}\frac{1}{\sqrt{D_c}(\gamma_0-1)}\left(\frac{e^{-x^2/D_c\theta}}{\sqrt{\pi}\sqrt{\theta}} - \sqrt{D_c}2\sum_{n=1}^{\infty}(-1)^n e^{-n^2\pi^2 D_c\theta}\cos[n\pi(1-x)] \right),$$

$$u(x,\theta) = \varphi\varepsilon\mu^{-\gamma-c+\alpha}\frac{2}{3}\sqrt{D_c}\left\{(1-x)\left[\frac{1}{\sqrt{\pi}\sqrt{\theta}/\mu^{\gamma-\alpha}} - (\gamma_0-1)\sqrt{D_c}e^{(\gamma_0-1)^2 D_c\theta/\mu^{2\gamma-2\alpha}}\operatorname{erfc}\left((\gamma_0-1)\sqrt{D_c}\frac{\sqrt{\theta}}{\mu^{\gamma-\alpha}}\right)\right]\right.$$

$$-\frac{e^{-x^2/\mu^{2(\gamma-\alpha)}/4D_c\theta/\mu^{2(\gamma-\alpha)}}}{\sqrt{\pi}\sqrt{\theta}/\mu^{\gamma-\alpha}} + (\gamma_0-1)\sqrt{D_c}e^{(\gamma_0-1)^2 D_c\theta/\mu^{2\gamma-2\alpha}+(\gamma_0-1)x/\mu^{\gamma-\alpha}}$$

$$\times\operatorname{erfc}\left.\left((\gamma_0-1)\sqrt{D_c}\sqrt{\theta}/\mu^{\gamma-\alpha}+\frac{x}{2\sqrt{D_c}\sqrt{\theta}}\right)\right\} + \varphi\varepsilon\mu^{\gamma-c+\alpha}\frac{2}{3}\frac{1}{\gamma_0-1}\left(\frac{xe^{-x^2/4D_c\theta}}{2\sqrt{D_c}\sqrt{\pi}\sqrt{\theta^3}} - 2\pi D_c\right.$$

$$\left.\times\sum_{n=1}^{\infty} e^{-n^2\pi^2 D_c\theta}(-1)^n\sin[n\pi(1-x)]\right),$$

$$p(x,\theta) = \frac{3}{2}(1+\mu) - \frac{9}{8} + \varphi\frac{3}{2}\left[1 - e^{(\gamma_0-1)^2 D_c\theta/\mu^{2\gamma-2\alpha}}i^0\operatorname{erfc}\left((\gamma_0-1)\sqrt{D_c}\frac{\sqrt{\theta}}{\mu^{\gamma-\alpha}}\right)\right] + \varphi\mu^{-\alpha+\gamma}\frac{3}{2}\frac{1}{\gamma_0-1}$$

$$\times\left(\frac{1}{\sqrt{\pi}\sqrt{D_c}\sqrt{\theta}} - 2\sum_{n=1}^{\infty} e^{-n^2\pi^2 D_c\theta}\right).$$

VII. CONCLUDING REMARKS

The present hydrodynamic theory of density relaxation in nearly supercritical fluids based on singular asymptotic expansion techniques gives a uniformly valid analytical description in space and time for fluid velocity, pressure, density, and temperature following a temperature step at the boundary. It confirms that the process driving density back to equilibrium involves two time scales, the short, piston effect time scale and the long, heat diffusion one. The matching procedure allows the initial conditions to be obtained for the long lasting density relaxation period. These initial conditions reflect the way the weakening piston effect gives place continuously to diffusion. The specific structure of the hydrodynamic field that was essentially thermally equilibrated by the piston effect involves a homogeneous bulk phase and a strongly mass-depleted area in the slightly hotter boundary region. It evolves diffusively and density relaxation is shown to be governed by a damped expansion-compression zone which slowly propagates in the bulk at the diffusion speed.

After this theory was completed, we observed that some earlier, unpublished measurements look like the present behavior. The generalization of the theory to real critical exponents also given in the paper allows for future data analysis or experimental investigation.

However, this description becomes invalid when the initial conditions are either far from the critical point [21] or nearer than a certain value [20]. Our theoretical efforts will thus be devoted to exploring these two limits. For the first, the initial conditions are far from the critical point so that the transport modes, i.e., adiabatic and entropy modes, are not yet fully separated in terms of time scales and thus make comparable contributions [21]. For the second, the initial conditions are very close to the critical point so that supercritical fluid hydrodynamics is driven by acoustic modes. Inside this close neighborhood of the critical point, puzzling mechanisms have been put forward theoretically, such as heat propagation at the speed of sound [20] or the inversion of acoustic wave reflection rules [22,23].

APPENDIX

Putting expansions (23) into the Navier-Stokes equations leads to the system of equations (24). The initial conditions are given by the limits for $\theta\to 0$ of the perturbations in Eqs. (22). These limits being singular, it is easier to perform the following change of variables:

$$\hat{p} = \tilde{p} - \frac{3}{2}\frac{1}{\gamma_0-1}\frac{1}{\sqrt{\pi}\sqrt{k_0}}\frac{1}{\sqrt{\theta}},$$

$$\hat{T} = \tilde{T} - \frac{1}{\sqrt{\pi}\sqrt{\kappa_0}}\frac{1}{\gamma_0-1}\frac{1}{\sqrt{\theta}}(1-e^{-x^2/4\kappa_0\theta}),$$

$$\hat{u} = \tilde{u} - \frac{1}{3}\frac{1}{\sqrt{\pi}\sqrt{\kappa_0}}\frac{1}{\gamma_0-1}\frac{1}{\sqrt{\theta^{3/2}}}xe^{-x^2/4\kappa_0\theta}),$$

$$\hat{\rho} = \tilde{\rho} - \frac{2}{3}\frac{1}{\gamma_0-1}\left(\frac{1}{\sqrt{\pi}\sqrt{\kappa_0}}\frac{1}{\sqrt{\theta}}e^{-x^2/4\kappa_0\theta} - 1\right),$$

which leads to the equations

$$\frac{\partial\hat{\rho}}{\partial\theta} + \frac{\partial\hat{u}}{\partial x},$$

$$\frac{\partial\hat{p}}{\partial x} = 0,$$

$$\frac{3}{2}\frac{\partial \hat{u}}{\partial x} - \kappa_0 \frac{\partial^2 \hat{T}}{\partial x^2} = \frac{t_0}{\gamma-1}\delta(\theta),$$

$$\hat{p} = \tfrac{3}{2}\hat{T} + \tfrac{9}{4}\hat{\rho},$$

with the initial boundary conditions

$$\theta = 0, \quad \hat{T} = \hat{\rho} = \hat{p} = \hat{u} = 0,$$

$$x = 0, \quad \hat{T} = \hat{u} = 0,$$

$$x = 1, \quad \frac{\partial \tilde{T}}{\partial x} = -\frac{1}{2\sqrt{\pi\kappa_0^3}}\frac{1}{\gamma_0-1}\frac{e^{-1/4\kappa_0\theta}}{\theta^{3/2}};$$

$$\hat{u} = -\frac{1}{3\sqrt{\pi\kappa}}\frac{1}{\gamma_0-1}\frac{e^{-1/4\kappa_0\theta}}{\theta^{3/2}}.$$

The singular behavior of the initial conditions has been transferred to the boundary conditions. The Laplace transform technique leads to the following system of equations:

$$m\hat{\rho} + \frac{\partial \hat{u}}{\partial x} = 0,$$

$$\frac{\partial \hat{p}}{\partial x} = 0,$$

$$\frac{3}{2}\frac{\partial \hat{u}}{\partial x} - \kappa_0 \frac{\partial^2 \hat{T}}{\partial x^2} = \frac{t_0}{\gamma-1},$$

$$\hat{p} = \tfrac{3}{2}\hat{T} + \tfrac{9}{4}\hat{\rho}.$$

After some algebra, the following solution is obtained in Laplace space:

$$\hat{T} = \frac{1}{\gamma_0-1}\frac{1}{\sqrt{\kappa_0}}\frac{1}{\sqrt{m}}\left(\frac{\cosh(\sqrt{m}/\sqrt{\kappa_0}(1-x))}{\sinh(\sqrt{m}/\sqrt{\kappa_0})} - \frac{\cosh(\sqrt{m}/\sqrt{\kappa_0})}{\sinh(\sqrt{m}/\sqrt{\kappa_0})}\right),$$

$$\tilde{\rho} = \frac{2}{3}\frac{1}{\gamma_0-1}\frac{1}{m}\left(\frac{\sqrt{m}}{\sqrt{\kappa_0}}\frac{\cosh[\sqrt{m}/\sqrt{\kappa_0}(1-x)]}{\sinh(\sqrt{m}/\sqrt{\kappa_0})}\right),$$

$$\tilde{p} = \frac{2}{3}\frac{1}{\gamma_0-1}\frac{1}{m}\left(\frac{\sqrt{m}}{\sqrt{\kappa_0}}\frac{\cosh(\sqrt{m}/\sqrt{\kappa_0})}{\sinh(\sqrt{m}/\sqrt{\kappa_0})}\right),$$

$$\tilde{u} = \frac{2}{3}\frac{1}{\gamma_0-1}\left((1-x) - \frac{\sinh[\sqrt{m}/\sqrt{\kappa_0}(1-\kappa)]}{\sinh(\sqrt{m}/\sqrt{\kappa_0})}\right).$$

The inversion of these with the aid of elementary tables gives the solution on the θ scale.

---

[1] A. Onuki, H. Hong, and R. A. Ferrel, Phys. Rev. A **41**, 2256 (1990).

[2] H. Boukari, J. N. Shaumeyer, M. E. Briggs, and R. W. Gammon, Phys. Rev. A **41**, 2260 (1990).

[3] B. Zappoli, D. Bailly, Y. Garrabos, B. le Neindre, P. Guenoun, and D. Beysens, Phys. Rev. A **41**, 2264 (1990).

[4] P. Guenoun, B. Khalil, D. Beysens, Y. Garrabos, F. Kammoun, B. Le Neindre, and B. Zappoli, Phys. Rev. E **47**, 1531 (1993).

[5] H. Klein, G. Schmitz, and D. Woermann, Phys. Rev. A **43**, 4562 (1991).

[6] Y. Garrabos, M. Bonetti, D. Beysens, T. Fröhlich, P. Carles, and B. Zappoli, Phys. Rev. E **57**, 5665 (1998).

[7] J. Straub, L. Eicher, and A. Haupt, Phys. Rev. E **51**, 5556 (1995).

[8] F. Zhong and H. Meyer, Phys. Rev. E **51**, 3223 (1995).

[9] R. A. Wilkinson, G. Zimmerly, H. Hao, M. R. Moldover, R. F. Berg, W. L. Johnson, R. A. Ferrel, and R. W. Gammon, Phys. Rev. E **57**, 436 (1998).

[10] A. Onuki and R. A. Ferrel, Physica A **197**, 245 (1990).

[11] F. Zhong and H. Meyer, Phys. Rev. E **53**, 5935 (1996).

[12] H. Boukari, R. L. Pego, and R. W. Gammon, Phys. Rev. E **52**, 1614 (1995).

[13] B. Zappoli, S. Amiroudine, P. Carles, and J. Ouazzani, J. Fluid Mech. **316**, 53 (1996).

[14] G. A. Zimmerly, R. A. Wilkinson, R. A. Ferrel, and M. R. Moldover (private communication).

[15] D. Beysens *et al.* (private communication).

[16] B. Zappoli, Phys. Fluids A **4**, 1040 (1992).

[17] S. Amiroudine, Ph. Larroude, P. Bontoux, and B. Zappoli, J. Fluid Mech. (to be published).

[18] B. Zappoli, A. Jounet, S. Amiroudine, and A. Mojtabi, J. Fluid Mech. **388**, 389 (1999).

[19] B. Zappoli and A. Durand Daubin, Phys. Fluids **6**, 1929 (1994).

[20] B. Zappoli and P. Carles, Physica D **89**, 381 (1995).

[21] D. Bailly and B. Zappoli (unpublished).

[22] B. Zappoli, P. Carles, S. Amiroudine, and J. Ouazzani, Phys. Fluids **7**, 2283 (1995).

[23] R. A. Ferrel and H. Hao, Physica A **197**, 23 (1993).